

Diffusion Bonding of Electroless Ni plated WC composite to Cu and AISI 316 Stainless Steel

AHMET YÖNETKEN¹, MEHMET ÇAKMAKKAYA¹, AYHAN EROL², ŞÜKRÜ TALAŞ^{2*},

¹ A. Kocatepe University, Technical Education Faculty, 03200, Afyonkarahisar, Turkey

² A. Kocatepe University, Faculty of Technology, 03200, Afyonkarahisar, Turkey

In this study, a composite containing WC (Tungsten Carbide) and Ni was produced by two different processing routes. Electroless Ni coated WC powders were consolidated and sintered at 1200 °C. Diffusion bonding couples of WC(Ni)-electrolytic Cu, WC(Ni)-AISI 316 stainless steel and WC(Ni)-WC(Ni) were manufactured by using a preloaded compression system under Ar atmosphere. Diffusion bonding was carried out at varying bonding temperatures; 750 °C for (WC)Ni-Cu diffusion couple and 1200 °C for (WC)Ni-(WC)Ni and (WC)Ni-AISI 316 stainless steel diffusion couples. Standard metallographic techniques, Scanning Electron Microscopy and a shear test were employed to characterize the microstructure of bondline and mechanical properties of each diffusion couple, respectively.

Keywords: *ceramic matrix composite, electroless plating, powder metallurgy, diffusion bonding*

© Wrocław University of Technology.

1. Introduction

Electroless Ni plating is a deposition process by which Ni metal ions are transferred onto non-reacting substrate by a reducing agent in the plating solution. It is widely used in aerospace, automotive and electronic industries [1]. To increase its applicability, electroless metal plating of many ceramics has been successfully employed to form a strong binding between particles of ceramics and thus utilize the superior wear and chemical corrosion properties of ceramic phase in highly demanding conditions [2–5]. The coating of WC powders has been studied for the electroless deposition of Ni and other metals, as well as Ni with P or B, and the electrolytic deposition of Ni onto WC particles and the effect of plating conditions with NiP have been also investigated [6–10]. The coating of WC with Co and Ni yields different results because Co coating decreases the friction between particles

more effectively than Ni coatings. Ni coating, on the other hand, provides better corrosion protection than Co and is superior to Co coatings in terms of mechanical performance [4, 5]. Diffusion bonding is a well known process for joining similar or different materials through the formation of bonds at atomic level with mating surfaces. The bonding is achieved as a result of closure of the voids at the interface of the mating surfaces, due to the local plastic deformation of asperities and interdiffusion of elements across the joint interface. Diffusion bonding of similar metals and ceramics is extensively performed and joining ceramics to metals was also investigated by the use of intermediate liquid phase, i.e. brazing, and others are produced by solid state diffusion bonding [11]. The joining of WC (Tungsten Carbide) plated by Ni by both transient liquid phase and direct bonding have also been attempted [12, 13]. In this study, electroless Ni plated WC powders were sintered and diffusion bonded to Cu and Stainless Steel(AISI 316) under the conditions of optimal bonding, and their mi-

*E-mail: stalas@aku.edu.tr

microstructure and mechanical properties were investigated using various characterization techniques.

2. Experimental Procedure

2.1. The production route for WC-Ni composite

WC powders of 99% purity with an average size of 20 μm were used and WC-Ni ceramic-metal composite was produced by electroless Ni plating of WC powders, followed by sintering at 1200 °C for 1h using a tube furnace. The WC(Ni) was fabricated so that it contained 70% WC and 30% Ni by weight.

Chemical Ni plating was achieved by suspending the starting WC powders in a Ni containing solution ($\text{NiCl}_2 \cdot 6\text{H}_2\text{O}$) at 95 °C and by adding Hydrazine Hydrate ($\text{N}_2\text{H}_4 \cdot \text{H}_2\text{O}$) and 35 vol.% Ammonia solution, while keeping the pH at 10. As the temperature increased, the Ammonia evaporation rate increased rapidly; therefore, a dripper was used for adding more ammonia in order to adjust the pH of the plating solution. In the mean time, the solution was continuously stirred and the pH was constantly monitored by using a Philips PW 9413 Ion-Activity Meter. The reaction was allowed to continue until sufficient Ni had been added for plating all the WC powders. Then, the Ni plated WC powders were filtered out of the solution by using a paper filter and repeatedly washed off by distilled water and then oven dried at 105 °C.

2.2. Diffusion bonding process and mechanical testing

Following the electroless coating of WC powders, powder mixtures were consolidated, with a single action die, into cubes of dimensions 6 mm x 8 mm x 12 mm. All opposing surfaces of diffusion couple specimens were ground, with abrasives up to 1000 Grit, perpendicular to the bondline prior to bonding. Diffusion bonding couples were aligned to fit and were compressed with a bonding load of 100 N at a temperature below melting point (750 °C for WC(Ni)-Cu (electrolytic) and 1200 °C for WC(Ni)-WC(Ni) and WC(Ni)-AISI 316 Stainless Steel). AISI 316 Stainless Steel typically con-

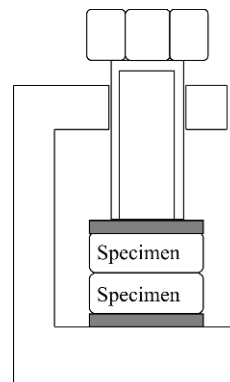


Fig. 1. The clamp used for diffusion bonding

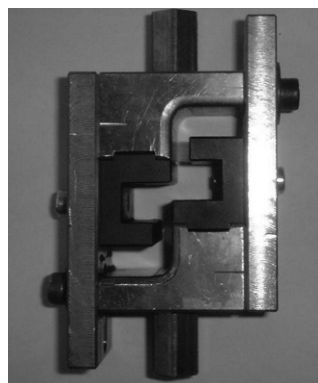


Fig. 2. The shear test apparatus for diffusion bonded specimens

tains 16-18 wt.% Cr and 10-14 wt.% Ni, 2-3 wt.% Mn and Mo and 0.08 wt.% C (max.). The diffusion bonding was performed in a vertical tube furnace with an Ar (Argon) atmosphere for 1/2 hr for all specimens using a clamp as shown in Fig. 1. The diffusion bonded specimens were allowed to cool down in the furnace after the bonding process. A sheet of WC was used on both sides of specimens in order to prevent sticking of specimens to the clamping surfaces.

The shear tests were carried out with the shear-strength testing apparatus shown in Fig. 2 using a Shimadzu AG-100 kN universal tensile testing machine with a crosshead speed of 0.05 mm/min at ambient temperature. The stress-strain curve was obtained following the mechanical testing and the shear strain and the shear stress values were taken from the point at which the fracture occurred on

the curve. Three specimens were tested for each series and average shear stress values and their error range were also calculated. The area that was exposed to shearing was 96 mm².

In Table 1, the experimental conditions for the diffusion bonding process are given; Cu, AISI 316 stainless steel and (WC)Ni composite combinations were compressed under appropriate load in the clamp. WC(Ni)-Cu diffusion couples were treated at lower temperature since Cu has a lower melting temperature than other components.

2.3. Microstructural characterization

Microstructural examination of the diffusion bondline was performed by LEO 1430 VP SEM (Scanning Electron Microscopy) equipped with Röntec EDS following the metallographic preparation. The optical images were taken after chemical etching by 1% vol. HF in alcohol after abrasive grinding of cross-sectional area 5 mm below the surface. For the SEM studies, the cross-sectional area of (WC)Ni-(WC)Ni diffusion bondlines were not polished but (WC)Ni-Cu and (WC)Ni-AISI 316 stainless steel specimens were used as prepared above. The average bondline width was determined by taking at least five measurements along the bondline in each specimen, between the points where the fully dense structures, i.e. fully compact and homogeneous metallic microstructures, were observed. EDS analysis of the selected area along the bondline was done by outlining a portion of interface between (WC)Ni and stainless steel or Cu.

3. Results and Discussion

The optical images from the diffusion bonded specimens are shown in Fig. 3. The diffusion bondline can be clearly seen in the ceramic-metal composites that were bonded with different materials. However, the bondline was not apparent when the (WC)Ni composite was diffusion bonded to itself.

Fig. 4 shows the diffusion bonded region from (WC)Ni-(WC)Ni diffusion couple. It is highly fractured along the bondline which contains fewer numbers of visible cracks, in both parallel and per-

pendicular directions. It also appears that the bondline has elongated voids which prevent the formation of good bonding between the specimens. The existence of voids, therefore, suggests that the bonding load should be increased if a seamless joint is to be obtained. The SEM image of the bondline of (WC)Ni-Cu diffusion bonded specimen is shown in Fig. 5. It can be seen that the diffusion bonding zone is wide and several WC particles are scattered along the bondline on the Cu side. Cu diffused extensively into the (WC)Ni composite, suggesting that the bonding is seamless. As seen in Fig. 6, the (WC)Ni-AISI 316 stainless steel diffusion couple bondline appears to be free of voids at the interface along which a seamless joint formation is achieved. It is interesting to note that, although the magnifications are the same, the (WC)Ni-AISI 316 stainless steel interface contains larger and less scattered WC particles.

The analysis of SEM images from the bondline of WC(Ni)-Cu and WC(Ni)-AISI 316 stainless steel (Figs 5 and 6), clearly shows that the particles were extensively engulfed by Cu and AISI 316 stainless steel thereby reducing the number of pores in WC(Ni) zone and as well as providing a strong binding between particles. The EDX spectrums from the selected area along the bondline of (WC)Ni-Cu and (WC)Ni-AISI 316 stainless steel specimen are given in Figs 7a and 7b. EDS analysis reveals that W, C, Ni, Cu and Cr were clearly identified within the bondline of each corresponding diffusion couple. It should also be noted that the amount of Ni is higher in the (WC)Ni-AISI 316 diffusion bondline than for the WC(Ni)-Cu sample, and the amount of W is clearly lower in the (WC)Ni-AISI 316 diffusion couple.

Table 2 shows the average width of the bondline for each diffusion couple. (WC)Ni-Cu diffusion bondline is wider compared with (WC)Ni-(WC)Ni and (WC)Ni-AISI 316 stainless steel bondlines. With the increased mass diffusivity at high temperatures, Ni on WC readily diffuses into Cu because of its complete solid solubility with the Cu lattice. This can be substantiated by taking diffusion rate constants into consideration, noting that the diffusion rate of Ni in Cu substrate is approximately

Table 1. Parameter values for the diffusion bonding experiment.

	Temperature (°C)	Load (N)	Time (min)
(WC)Ni-Cu	750	100	30
(WC)Ni-AISI 316	1200	100	30
(WC)Ni-(WC)Ni	1200	100	30



Fig. 3. The diffusion bonded specimens of (WC)Ni-AISI316, (WC)Ni-Cu and (WC)Ni-(WC)Ni (from left to right)

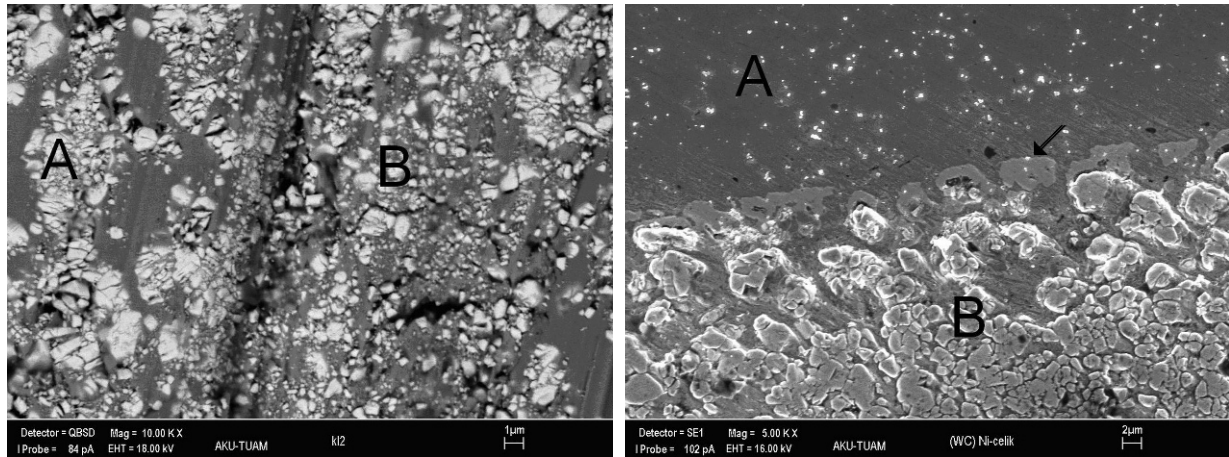


Fig. 4. (WC)Ni-(WC)Ni diffusion bondline; A and B are both (WC)Ni

Fig. 6. WC(Ni)-AISI316 diffusion bondline; A: AISI316 stainless steel and B: (WC)Ni

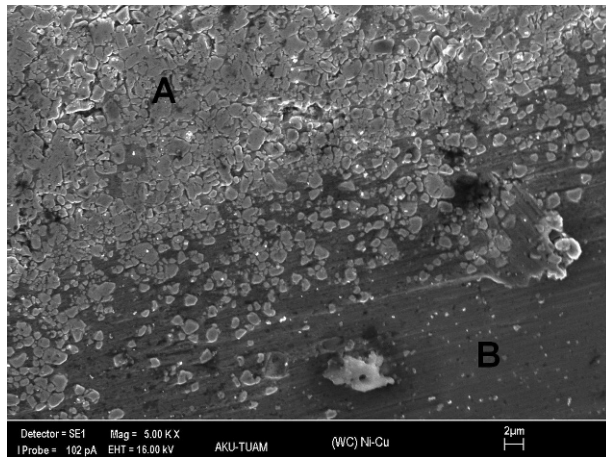


Fig. 5. (WC)Ni-Cu diffusion bondline; A: (WC)Ni and B: Cu

Table 2. Average width of the bondline in diffusion bonded material couples.

Specimen	Average width of the bondline (μm)
WC(Ni)-WC(Ni)	8.5 ± 0.6
WC(Ni)-Cu	22.8 ± 0.8
WC(Ni)-AISI 316	12.6 ± 0.3

$1,98 \cdot 10^{-13} \text{ m}^2/\text{s}$ as opposed to $4,1 \cdot 10^{-15} \text{ m}^2/\text{s}$ for Cu in Ni substrate [14], but as the formation of Ni-Cu alloy takes place the diffusion rate of Cu increases to $1,58 \cdot 10^{-14} \text{ m}^2/\text{s}$, allowing the rapid mass transfer of Cu to be relatively faster compared with the Ni rich corner of the Cu-Ni phase diagram [15]. In other words, the diffusion process

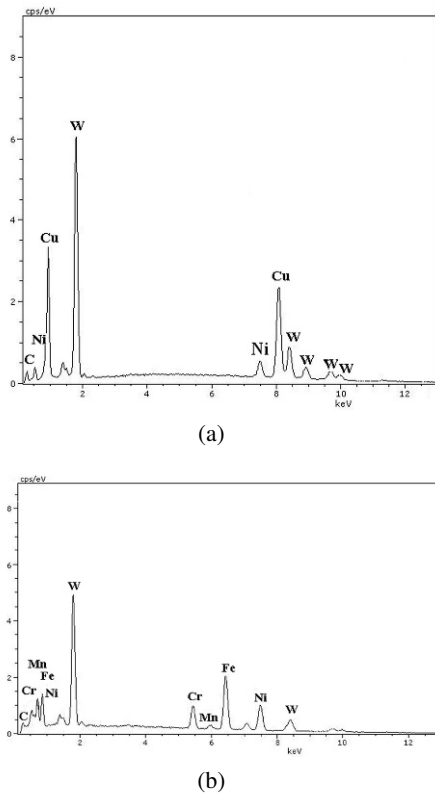


Fig. 7. The EDX spectrum showing the bondline composition of a) (WC)Ni-Cu b) (WC)Ni-AISI 316 stainless steel diffusion couple

in the (WC)Ni-Cu bondline is dictated by the diffusion rate of Ni in Cu substrate, but it should also be noted that Ni layer on WC particles forms NiCu solid solution in the vicinity of WC particles, and hence the diffusion process slows down due to the reduced diffusion rate. Nevertheless, it is obvious that the diffusion rates of Ni and Cu are not the sole factors affecting the width of the bondline: other processes such as mass deformation of the bondline should also be contributory factors. High mass diffusivity may also be observed with the (WC)Ni-AISI 316 diffusion couple, because of the complete solubility of Ni in Cr up to 46 wt% of Cr. However, the complete solubility of Ni in Cr ceases at 46 wt% of Cr and a two phase zone of f.c.c. (Ni) and b.c.c. (Cr) is formed [16]. In a WC(Ni)- AISI 316 stainless steel diffusion couple, the higher initial Ni content at the contacting surfaces gradually decreases under alloying of Ni by Cr and Fe in

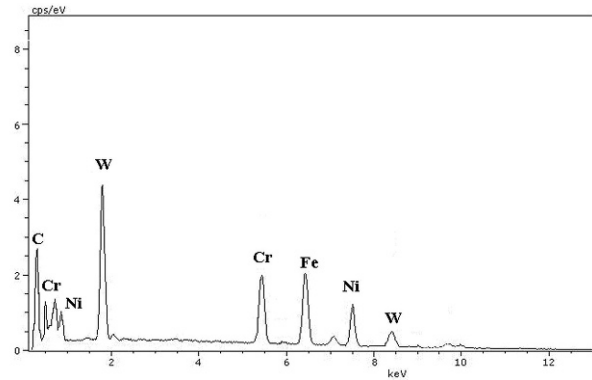


Fig. 8. A spot analysis from an interface in the vicinity of WC at (WC)Ni-AISI316 bondline (Grey zone indicated by arrow in Fig. 6)

AISI 316, but as the Cr comes into greater contact with C in WC compound, conditions at the interface become more favourable for the the formation of Cr_3C_2 or (W,Cr)C type of carbides [17]. Indeed, as can be seen in Fig. 8, the spot analysis of a grey zone indicated in Fig. 6, (WC)Ni-AISI 316 diffusion bondline, suggests that a carbide containing W and Cr can form in the vicinity of electroless Ni coated WC particles. It is also possible that a ternary solid solution containing Fe, Ni and Cr may have formed near Ni coated particles. Nevertheless, the formation of two phases at higher ratios of Cr and Ni can also impede the advancement of the diffusion front by Cr and Fe, as the diffusion activity is dictated by the nucleation and growth of α and γ phases [17, 18]. One should also be aware that AISI 316 surface asperities are not as easily deformable as surface asperities on Cu surfaces, preventing the formation of a wider bondline as in the (WC)Ni-Cu bondline. Such complications may result in a lower average width of bondline, as shown in Table 2, except for the WC(Ni)-WC(Ni) diffusion couple. For the WC(Ni)-WC(Ni) diffusion couple, a lower average width of bondline may be the result of lower contents of highly diffusing metal atoms within the highly fractured WC particles situated at the interface.

The shear stress (τ) values of the samples are given in Table 3. It can be seen that the highest shear stress was observed with (WC)Ni-Cu diffusion couple as 48,3 MPa and the lowest stress was

Table 3. Shear stress values for the diffusion bonded specimens.

Diffusion bonded specimens	Shear Stress, τ (MPa)	Shear strain, γ (%)
(WC)Ni/Cu	48.3±2.1	4.4
(WC)Ni/ AISI 316	39.7±3	2.1
(WC)Ni/(WC)Ni	30.2±2.6	0.9

observed for WC(Ni)-WC(Ni). The shear stress results in Table 3 appear to be consistent with a similar trend regarding the average width of the bondline, because there is a direct relationship between the quality of the bondline and the strength. During the shear testing of the (WC)Ni-(WC)Ni diffusion couple, the amount of plastic deformation was gradually increased: when the compression load attained the maximum (critical) value for the given sample, a crack occurred on the specimen and a visible displacement, due to fracture along the height of the sample, could be seen. Following the formation of a crack at the diffusion bondline, the stress values dropped back to zero without extensive physical rupturing of the specimens. (WC)Ni-(WC)Ni diffusion couple specimens yielded stress values similar to their compression test results for specimens sintered at 900 °C [19]; it appears that there is a strong correlation between the width and shear stress of the corresponding diffusion bondline in question. The lower stress values for the (WC)Ni-(WC)Ni diffusion couples are obviously due to the presence of cracks at or near the bondline. However, the (WC)Ni-AISI316 diffusion couple also yielded a comparatively lower shear stress, probably due to the formation of hard phases in the bondline and narrow bondline width. The latter may influence the amount of shearing volume and result in the shearing of a higher volume of (WC)Ni. For the (WC)Ni-Cu diffusion couple, the relatively higher shear stress is due to an increased shearing volume of the bondline with evenly distributed WC particles, despite the low shear strength of Cu [20].

4. Conclusions

The diffusion bonding of WC(Ni) composite to itself, to electrolytic copper and to Stainless Steel

(AISI 316 grade) was successfully carried out under an Ar atmosphere in a tube furnace under a load of 10N. The results suggest that diffusion bonded WC(Ni)-Cu specimens have higher diffusion bonding capability over WC(Ni)-WC(Ni) and WC(Ni)-AISI 316 stainless steel diffusion bonded couples, when taking into consideration both the mechanical performance and the metallographic examination of bondlines of each specimen. It is believed that Cu quickly diffuses into the Ni matrix and forms a solid solution which eases the formation of sound bondlines, whereas Fe and Cr may slow down the diffusion process at the interface, due to the formation of carbides, and reduce the average diffusion width at the bondline.

References

- [1] HENRY J.R., *Met. Finish*, 97 (1999), 424.
- [2] WU P., DU H.M., CHEN X.L., LI Z.Q., BAI H.L., and JIANG E.Y., *Wear*, 257 (2004), 142.
- [3] FARROQ T., and DAVIES T.J., *Int. J. Powder Metall.*, 27 (1991), 347.
- [4] STRAFFORD K.N., DATTA P.K., and O'DONNELL A.K., *Mater. Design*, 3 (1982), 608.
- [5] GUOZHI X., JINGXIAN Z., YIJUN L., KEYU W., XIANGYIN M., and PINGHUA L., *Mater. Sci. Eng. A*, 460 (2007), 461.
- [6] BALARAJU J.N., NARAYANAN T.S.N.S., and SEHADRI S.K., *J. Appl. Electrochem.*, 33 (2003), 1241.
- [7] GIAMPAOLO A.R., ORDONEZ J.G., GUGLIEMACCI J.M., and LIRA J., *Surf. Coat. Tech.*, 89 (1997), 127.
- [8] STROUMBOULI A., GYFTOU P., PAVLATOU E.A., and SPYRELLIS N., *Surf. Coat. Tech.* 195 (2005), 325.
- [9] HAMID Z.A., EL BADRY S.A., and AAL A.A., *Surf. Coat. Tech.* 201(2007), 5948.
- [10] FERNONDES C.M., SENOS A.M.R., CASTANIO J.M., and VIEIRA M.T., *Mater. Sci. Forum*, 514-516 (2006), 633.
- [11] LEMUS-RUIZ J., CEJA-CÁRDENAS L., VERDUZCO J.A., and FLORES O., *J. Mater. Sci.*, 43 (2008), 6296.
- [12] KURT A., UYGUR I., and ATES H., *Mater. Sci. Forum*, 546-549 (2007), 667.
- [13] LU S-P., KWON O-Y., *Surf. Coat. Tech.*, 153 (2002), 40.

-
- [14] BUTRYMOWICZ D.B., MANNING J.R., and READ M.E., Diffusion Rate Data and Mass Transport Phenomena for Copper Systems, National Bureau of Standards, Washington, 1977.
- [15] Cu-Ni phase diagram, www.calphad.com.
- [16] Ni-Cr phase diagram, www.calphad.com.
- [17] BRIESECKA M., BOHNB M., LENGAUERA W., J. Alloy Comp., 489 (2010), 408.
- [18] Fe-Cr phase diagram, www.calphad.com.
- [19] YONETKEN A., PhD Thesis, Afyon Kocatepe University, Institute of Natural Sciences, 2008 (in Turkish).
- [20] MEYERS M.A., CHAWLA K.K., Cambridge University Press, Cambridge, 2009.

Received 29.01.2010

Accepted 09.11.2010